Arab J Sci Eng (2013) 38:1115–1130
DOI 10.1007/s13369-012-0534-5

RESEARCH ARTICLE - MECHANICAL ENGINEERING

Fundamental Basis and Application of Cold-Room Project Design: A Turkish Case Study

A. S. Dalkilic · N. A. Kurekci · O. Kincay · S. Wongwises

Received: 26 March 2011 / Accepted: 2 May 2011 / Published online: 10 January 2013
© King Fahd University of Petroleum and Minerals 2013

Abstract In this paper, cold-room systems in Turkey's various regions were analyzed as case studies to demonstrate the application of the proposed model. They were also compared with each other in terms of the alteration of alternative refrigerants and insulation thickness and energy and exergy analyses of the cold rooms' refrigeration system. The coefficients of performance (COP), refrigerant charge rates, volumetric refrigeration capacity and capacities of each component of the refrigeration system for the refrigerants CFC-12, HCFC-22 and their alternatives, such as HFC-134A, HFC-404A, HFC-407C, HFC-410A and HFC-507, were determined by considering the effects of the main parameters of the performance analysis, such as refrigerant type, degree of subcooling, superheating and compressor efficiency. The first law efficiencies, exergy efficiencies and irreversibility rates were also obtained and discussed in this theoretical study. Based on the results of the energy analyses, all the alternative refrigerants have a slightly lower COP and require lower refrigerant charge rates than CFC-12 and HCFC-22 for condensation temperatures ranging from36–47 °C. The investigated large cities in Turkey have an evaporation temperature of −6 °C regarding the preserved product and various ambient temperatures of these largest cities of Turkey range from 31–42 °C in the case studies. Based on the results of the exergy analyses, the compressor has the greatest irreversibility, followed by the expansion valve, condenser and evaporator as the components of the refrigeration system.

Keywords Cold room · Heat transfer · Refrigerant · Exergy · Case study

الخلاصة

تم - في هذه الورقة العلمية- تحليل نظم الغرفة الباردة في مناطق مختلفة في تركيا ودراسة الحالة لبيان تطبيق الأنموذج المقترح. وتمت أيضا مقارنة بعضها ببعض من حيث تغيير غازات التبريد البديلة ، وسمك العزل، وتحاليل الطاقة ، والطاقة القصوى في نظام تبريد الغرفة الباردة. وتم إيجاد معاملات الأداء (COP)، ومعدلات شحن المبردات، وقدرة التبريد الحجمي، وقدرات كل عنصر من عناصر نظام التبريد لمبردات CFC-12، 22- HCFC وبدائلها، مثل A134-HFC، A404-HFC، C407 -HFC، A410 HFC و507-HFC ، وذلك من خلال النظر في الآثار المترتبة على المعالم الرئيسية لتحليل الأداء، مثل نوع المبردات، ودرجة التبريد الجزئي، والتسخين الفائق ، وكفاءة الضاغط. كما تم الحصول على كفاءات القانون الأول، و كفاءة الطاقة القصوى ، ومعدلات الرجعة ومناقشتها في هذه الدراسة النظرية. وبناء على نتائج تحليلات الطاقة فإن كل من المبردات البديلة لها COP أقل قليلا، وتتطلب معدلات شحن المبردات أقل من-CFC 12 و HCFC 22- لحرارات تكثيف تمتد من 36 مئوية إلى 47 مئوية. إن المدن الكبيرة في تركيا التي تم التحقيق فيها لديها درجة حرارة تبخر -6 مئوية بشأن المنتج المحافظ عليه ودرجات الحرارة المحيطة المختلفة لهذه المدن الكبرى في تركيا التي تمتد من 31 إلى 42 مئوية في دراسات الحالة. وبناء على نتائج تحاليل الطاقة القصوى فإن الضاغط لديه أكبر لا رجعة، يليه صمام التوسع، والمكثف والمبخر ومكونات نظام التبريد.

A. S. Dalkilic (✉) · N. A. Kurekci · O. Kincay
Heat and Thermodynamics Division,
Department of Mechanical Engineering,
Yildiz Technical University, Yildiz, Besiktas,
Istanbul 34349, Turkey
e-mail: dalkilic@yildiz.edu.tr

S. Wongwises (✉)
Fluid Mechanics, Thermal Engineering
and Multiphase Flow Research Lab. (FUTURE),
Department of Mechanical Engineering,
Faculty of Mechanical Engineering,
King Mongkut's University of Technology Thonburi,
Bangmod, Bangkok 10140, Thailand
e-mail: somchai.won@kmutt.ac.th

Abbreviations

A	Area, m^2
CFCs	Chlorofluorocarbons
COP	Coefficient of performance
C_{p1}	Specific heat for the temperature above the freezing temperature, J kg^{-1} K^{-1}
C_{p3}	Specific heat for the temperature after freezing process, J kg^{-1} K^{-1}
E	Exergy rate, kW
e	Specific exergy, kJ kg^{-1}
E_Q	Rate of exergy of heat input, kW
E_W	Rate of exergy of power output, kW
F	Defrost factor
GWP	Global warming potential
h	Enthalpy, kJ kg^{-1}
h_i	Inner convective heat transfer coefficient, W m^{-2} K^{-1}
h_d	Outer convective heat transfer coefficient, W m^{-2} K^{-1}
H_d	Air alteration coefficient
HCFCs	Hydro chlorofluorocarbons
HCs	Hydrocarbons
HFCs	Hydro fluorocarbons
I	Rate of irreversibility, kW
k	Thermal conductivity, W m^{-2} K^{-1}
K	Total heat transfer coefficient, W m^{-2} K^{-1}
L	Length, m
l	Freezing heat of product, W kg^{-1}
m	Mass flow rate, kg s^{-1}
m_e	Exergy flow rate of working fluid, kg s^{-1}
m_p	Mass of product, kg
n_{eh}	Total number of electric heaters in the cold room
n_{em}	Total number of electric motors in the cold room
n_p	Total number of people in the cold room
ODP	Ozone depletion potential
P	Pressure, MPa
R	Refrigerant
s	Entropy, kJ kg^{-1} K^{-1}
Q	Heat rejection rate, kW
Q_i	Heat generation of a person, kW
T	Temperature, °C or K
T_0	Environmental reference temperature, °C or K
t_{41}	Total working duration of people in the cold room, h
t_{42}	Illumination time for a day, h
t_{43}	Total working time of an electric motor, h
W	Isentropic compression work, kNm kg^{-1}
W_1	Power of illumination, kJ
W_2	Power of electric motors, kJ
W_3	Power of electric heaters, kJ
ΔT	Temperature difference, K

Greek Symbols

ρ	Density, kg m^{-3}
η	Efficiency
δ	Efficiency defects

Subscripts

afp	After freezing point of product
cl	Ceiling
CL	Cooling load
CR	Cold room
comp	Compressor
cond	Condensing/condenser
E	Exergy
evap	Evaporating/evaporator
fl	Floor
fp	Freezing point
gen	Generation
in	Inside
out	Outside
T	Total
tv	Throttling valve
1	Evaporator superheat
2	Compressorsuperheat
3	Condensersaturated liquid
4	Evaporator saturated mixture

1 Introduction

The refrigeration process is the main process of cold-room systems, which provide proper preservation temperatures to preserve the quality of products. The product is usually a type of perishable food within a certain isolated volume. In addition, many types of medical and perishable products are stored in the same way. It is important for designers to pay attention to the cooling load and the freezing temperatures, which prevent the growth of bacteria. Further, they should know the correct and appropriate type of compressor and condenser to be used in the cold-room system in advance. There are numerous details to plan at the design stage, such as efficient cold-storage space, its location with regard to transportation time from the cold room to the market area, product types stored together at the same time, building materials and seasonal temperature changes of its location.

Many investigations have conducted research on substitutes for CFC-12 and CFC-22. Chlorine atoms cannot be contained in the chemical structure of candidate refrigerants due to their harmful effects, such as ozone layer depletion and global warming. Since the discovery of the depletion of the earth's ozone layer and as a result of the 1992 United

Nations Environment Program meeting, the use of CFC-11 and CFC-12 has been phased out. They were used primarily in conventional refrigeration and air conditioning equipments. Besides this, HCFCs is expected to be prohibited after 2030 [1]. HFC-134A and HFC-152A were proposed as replacements of CFC-12 by the American Household Appliances Manufacturers (AHAM) [2]. They can be used as alternative refrigerants in domestic refrigeration due to their specifications of non-toxicity, flammability classes as A1 for R134A and A2 for R152A, and better ozone-depleting potential (ODP) and global-warming potential (GWP). The commercial refrigerant propane/isobutane blends have been utilized in small systems as substitutes for CFC-12 in recent years. Moreover, R407C is acceptable as a short-term replacement for R22 due to its having similar properties to R22.

Wongwises et al. [3] performed an experimental study on the application of hydrocarbon mixtures to replace HFC-134A in automotive air conditioners. The hydrocarbons investigated were propane (R290), butane (R600) and isobutane (R600A). The measured data were obtained from an automotive air conditioning test facility that utilized HFC-134A as the refrigerant. Wongwises and Chimres [4] conducted an experimental study on the application of a mixture of propane, butane, and isobutene to replace HFC-134A in a domestic refrigerator. The results showed that a 60/40 propane/butane mixture was the most appropriate alternative refrigerant. Wongwises and Pirompak [5] reported the results of simulations using an adiabatic capillary tube model developed to study the flow characteristics in adiabatic capillary tubes used as control devices in refrigerating systems and validated by the usage of alternative refrigerants and their mixtures. Wongwises et al. [6] presented a theoretical comparison of the flow characteristics of numerous pairs of refrigerants flowing through adiabatic capillary tubes. For all pairs, numerical results showed that the traditional refrigerants consistently gave lower pressure drops for both single-phase and two-phase flow than the environmentally acceptable alternative refrigerants, which resulted in longer tube lengths. Dalkilic and Wongwises [7] performed a theoretical performance study on a traditional vapor compression refrigeration system with refrigerant mixtures based on HFC-134A, HFC-152A, HFC-32, HC-290, HC-1270, HC-600 and HC-600A for various ratios. They compared their findings with CFC-12, CFC-22, and HFC-134A as possible alternative replacements. Results showed that all the alternative refrigerants investigated in the analysis had a slightly lower performance coefficient (COP) than CFC-12, CFC-22 and HFC-134A. Dalkilic and Wongwises [8] compared a single-stage vapor compression refrigeration system with an actual vapor compression cycle, a single-stage process with an internal heat exchanger and a two-stage process with an economizer using HCFC-22 and CFC-502 and their alternatives, such as HFC-134A, HFC-32, HFC-152A, HFC-404A, HFC-407C, HFC-507 and HFC-410A. Some of the alternative refrigerants' COP values were found to be higher than those of their base traditional pure refrigerants. The effects of the main parameters of the performance analysis, such as refrigerant type, degree of subcooling and superheating on the performance coefficient, refrigerant charge rate and volumetric refrigeration capacity, were investigated for various operating conditions as case studies. Dalkilic [9] presented a comparison of CFC-12, HCFC-22, CFC-502 and their alternatives, such as HFC-134A, HFC-152A, HFC-404A, HFC-407C, HC-290, HC-600A, R717 (ammonia) and three mixtures composed of HFC-134A, HFC-152A, HC-600A and HC-290. His theoretical performance study on a cascade refrigeration system was conducted using two refrigeration cycles connected through a heat exchanger in the middle of the cycle working as an evaporator for the high-pressure cycle and a condenser for the low-pressure cycle. The separate usage of R717 and HFC-152A for the high-pressure and low-pressure sections of the cascade system, respectively, was found to be superior in the analysis to determine the COP and refrigerant charge rates.

Exergy can be defined as a potential or quality of energy. Based on a review of the literature, it seems that the determination of a sustainable quality assessment of energy is possible. There is a relationship among the laws of thermodynamics and exergy. There are specific applications that require the simultaneous calculation of exergy and energy. Dopazo et al. [10] investigated a cascade refrigeration system with CO_2 and NH_3 as working fluids in the low- and high-temperature stages, respectively. Determinations of COP and exergetic efficiency and optimization studies based on the optimum CO_2 condensing temperature have also been performed. Lee et al. [11] used CO_2 and R717 in a cascade refrigeration system to determine the optimal condensing temperature of the cascade condenser, given various design parameters, to maximize the COP and minimize the exergy destruction of the system. They found that the maximum COP increased with evaporating temperature, but decreased as the condensing temperature or temperature difference between the brine and the refrigerant increased. Kanoglu [12] performed an exergy analysis of the multistage cascade refrigeration cycle used for natural gas liquefaction. The equations of exergy destruction and exergetic efficiency for the main cycle components, such as evaporators, condensers, compressors and expansion valves, were developed in his study.

In this study, a single-stage vapor compression refrigeration cycle for some well-known pure refrigerants was investigated to conduct energy and exergy analyses of the cycle at various insulation thicknesses (i.e., 75, 100 and 125 mm) and condenser and evaporator temperatures, according to the largest cities of Turkey in different climatic regions. Graphical presentations are shown to determine high-performance

Table 1 Outside design temperatures in summer in the investigated cities of Turkey [16,17]

City	Dry-bulb thermometer temperature (°C)	Wet-bulb thermometer temperature (°C)	Soil temperature (°C)
Erzurum	31	23	15
İstanbul	33	24	20
Ankara	35	21	20
Antalya	39	28	25
Diyarbakır	42	23	25

refrigerants for the preserved product's specified evaporating temperature of −6 °C. Also, condensing temperatures ranged from 36–47 °C, and the various ambient temperatures of Erzurum, Istanbul, Ankara, Antalya and Diyarbakır ranged from 31–42 °C in the cycle. In addition, the fundamental basis and application of cold-room project design are discussed as a sample case study for the simulation of a cold room under specified operating conditions (see Table 1). Accordingly, the main aim of this study was to analyze the single-stage refrigeration cycle to show the differences in refrigeration system components' capacities based on the specified preserved product and various refrigerants. Thus, the use of less energy for the refrigeration system can be obtained and efficiency can be increased by determining the total irreversibility rates and rational efficiency values as a result of the analyses. The specifications of low potentials of ODP and GWP make investigated refrigerants preferable for use in actual refrigeration systems.

2 Theoretical Computation Model

The ideal refrigeration cycle [13] shown in Fig. 1 was considered for the working substances that changed phases during the cycle. Actual refrigeration cycle systems have some deviations from the ideal one due to actual pressure losses due to fluid flow and heat transfer exchange in the surroundings. Cycle performance determination is performed to ease theoretical calculations by means of several assumptions: steady-state operating conditions, negligible alterations of kinetic and potential, an adiabatic (well-insulated) heat exchanger, saturated liquid at the outlet of the condenser, saturated vapor at the inlet of the compressor, neglect of pressure drops and heat loss in the environment from evaporators and condensers (see Fig. 1a), isenthalpic flow across the expansion valves and the assumed isentropic efficiency for the compressor. Theoretical investigations were performed using REFPROP [14] and SOLKANE [15] to determine the related physical properties of the refrigerant cycle states in accordance with the various refrigerants. The superheated state of vapor exists at the inlet of the compressor (see Fig. 1b). The pressure of the liquid at the outlet of the condenser is lower than the pressure

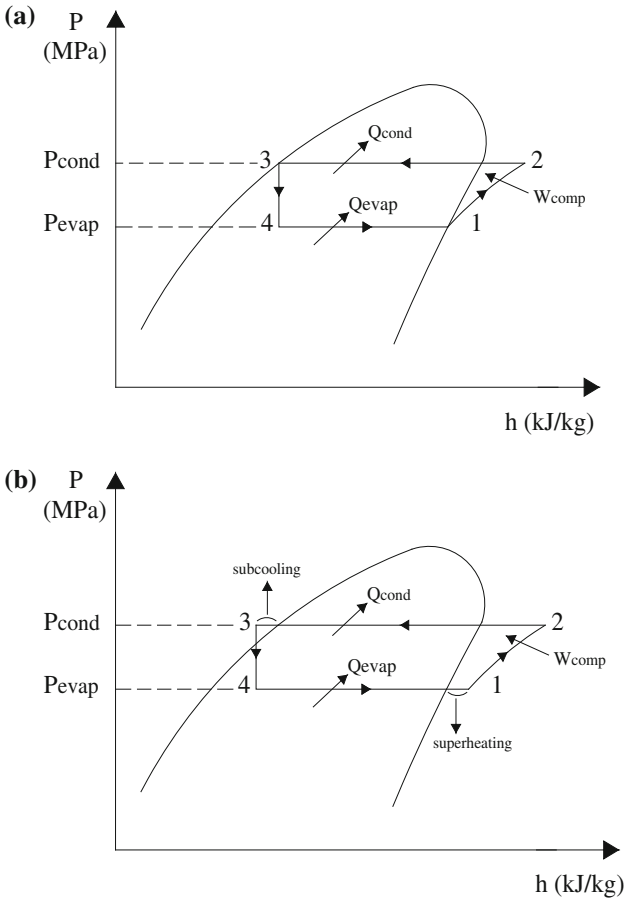


Fig. 1 The ideal vapor-compression refrigeration cycle **a** with P-h diagram **b** for the performance analysis of alternative refrigerants

at the inlet. In addition, there is a greater-than-ideal pressure drop between the condenser and the expansion valve, whereas a larger pressure drop occurs in the evaporation line in actual systems.

2.1 Case Study

In this study, the cold room was used for storing 100,000 kg of pears, requiring preservation at a temperature of –1 °C (−1.6 ÷ –0.5 °C), as recommended by the Intervention Board for Agricultural Products in Turkey. The cold room's dimensions were 14 × 18 × 4.5 m^3 (1,134 m^3) for the preserved product in terms of the planning of efficient preservation conditions in the room considering the product blocks and forklift turnings. The relative humidity of the cold room was set at 90 % for pear preservation (90–95 %). The temperature difference between the cold room and the evaporator was assumed to be 5 K. The evaporator's steady-state temperature was fixed at −6 °C in terms of the preserved products. The ambient temperatures were selected for the investigated cities, such as 31, 33, 35, 39 and 42 °C. Further, the saturation temperatures of the

Table 2 The detailed specifications of the construction materials of the cold room

Material	L (m)	k ($W m^{-1} K^{-1}$)	h_i ($W m^{-2} K^{-1}$)	h_d ($W m^{-2} K^{-1}$)	K ($W m^{-2} K^{-1}$)
Outer walls					
Tile	0.01	0.78	9	23	0.32
Internal plastering	0.02	0.87			
Hollow brick	0.23	0.45			
Polyurethane	0.1	0.041			
External plastering	0.03	1.4			
Inner walls					
Tile	0.01	0.78	9	9	0.31
Internal plastering	0.02	0.87			
Hollow brick	0.23	0.45			
Polyurethane	0.1	0.041			
External plastering	0.03	1.4			
Floor					
Terrazzo tile	0.035	1.05	8	∞	0.33
Cement finish	0.03	1.4			
Lean concrete	0.2	1.2			
Polyurethane	0.1	0.041			
Lean concrete	0.2	1.2			
Blockage	0.15	1.74			
Ceiling					
Internal plastering	0.02	0.87	6	23	0.31
Polyurethane	0.1	0.041			
Beton	0.2	0.65			
Asphalt insulation	0.03	0.13			
Door					
Sheet iron (2 pieces)	0.004	46.5	9	23	0.56
Fagus	0.04	0.2			
Polyurethane	0.05	0.041			
Fagus	0.04	0.2			

condenser were calculated as 36, 38, 40, 44 and 48 °C. All assumptions regarding the investigated cities and preserved products were obtained from Duruk and Sarıbatı [16], whereas the conditions of Turkey were acquired from Özkol [17].

The system's cooling load was calculated by means of heat gained from all surfaces and the preserved products in the cold room as shown in Eq. (1). The cold room's heat gained per hour was the sum of the following heat transfer rates: the heat transfer rate from the walls surrounding the cooled volume, ceiling and floor; the heat transfer rate from air alterations; the heat transfer rate from the preserved products and the heat transfer rate from the heat sources in the cold room. The unknown heat gains were usually considered as shown in Eq. (2). A 10 % increase was added to the total value of the system's cooling load, which was equal to the evaporator's heat rejection rate from the cold room. The heat gains can be calculated respectively as follows:

$$Q_T = Q_{11} + Q_{12} + Q_{13} + Q_{21} + Q_{31} + Q_{32} + Q_{33} + Q_{34} + Q_{41} + Q_{42} + Q_{43} + Q_{44} \quad (1)$$

$$Q_{CL} = 1.1 Q_T \quad (2)$$

The total heat transfer coefficient was calculated using Eq. (3) as follows

$$\frac{1}{K} = \frac{1}{h_i} + \sum_{i=1}^{n} \frac{L_i}{k_i} + \frac{1}{h_d} \quad (3)$$

The total heat transfer coefficient in Eqs. (4, 6, 8) was modified according to the manner of heat loss for the walls, floor, ceiling and door. Their construction materials are shown in Table 2 for the insulation material with 100-mm thickness. The temperatures of the cold-room system were considered with a machine room ($T_{out} + 5$ °C), an entrance (T_{out}) and an office ($T_{out} - 8$ °C). The floor (T_{soil}) and the ceiling ($T_{out} - 5$ °C) were examined according to the dry bulb temperature

Table 3 Infiltration rates to be added to the outside temperature due to the effect of sun light [16,17]

Way/color	East	South	West	Plan glass
Dark	4	3	4	10
Normal	3	2	3	8
Light	2	1	2	5

of the investigated cities (T_{out}) in Table 1. Whereas the temperature differences in these equations were calculated by means of the related neighbor volumes' temperatures, the infiltration rates from the sun light (see Table 3) were added to the outside temperature (T_{out}).

2.1.1 Heat Transfer Rate from the Walls (Q_{11})

The heat transfer rate from the total wall surfaces was determined for the inner and outer walls, whose directions were north, east, south and west, separately. The average heat conduction coefficient of the cold room's walls was calculated as follows:

$$Q_{11} = A_{out} K_{out} \Delta T_{11} \tag{4}$$

where the temperature difference was the difference between the inside and outside temperatures.

$$\Delta T_{11} = T_{out} - T_{in} \tag{5}$$

In addition, the value of the average heat conduction coefficient was usually between 0.3 and 0.6 $W\,m^{-2}\,K^{-1}$

2.1.2 Heat Transfer Rate from the Floor (Q_{12})

The heat gained from the floor of the cold room was calculated in a similar way as that from the walls of the cold room:

$$Q_{12} = A_{fl} K_{fl} \Delta T_{12} \tag{6}$$

where the temperature difference was the difference between the floor and inside temperatures.

$$\Delta T_{12} = T_{fl} - T_{in} \tag{7}$$

2.1.3 Heat Transfer Rate from the Ceiling (Q_{13})

The heat gained from the outside to the inside of the cold room related to the surface of the ceiling was determined as follows:

$$Q_{13} = A_{cl} K_{cl} \Delta T_{13} \tag{8}$$

Table 4 Sample case study for the comparison of various refrigerants with the insulation thickness of 100 mm for the different cities at $T_{CR} = -1\,°C$, $T_{evap} = -6\,°C$, $\Delta T_{subcooling} = 0\,°C$, $\Delta T_{superheating} = 0\,°C$ and $\eta_{comp} = 1$

City	Refrigerant	h_1 (kJ kg^{-1})	h_2 (kJ kg^{-1})	h_3 (kJ kg^{-1})	h_4 (kJ kg^{-1})	h_5 (kJ kg^{-1})	h_6 (kJ kg^{-1})	m (kg h^{-1})	Q_{evap} (kW)	Q_{cond} (kW)	W_{comp} (kW)	COP
Diyarbakır $T_{out} = 42\,°C$ $T_{cond} = 47\,°C$	R12	350.77	377.88	377.88	246.47	246.47	350.77	1455.88	42.18	53.14	10.96	3.85
	R22	402.65	440.33	440.33	258.95	258.95	402.65	1056.7	42.18	53.24	11.06	3.81
	R134a	394.97	429.39	429.39	266.93	266.93	394.97	1185.94	42.18	53.52	11.34	3.72
	R407c	406.57	445.89	445.89	263.79	263.79	406.57	1063.51	42.18	53.80	11.62	3.63
	R410A	419.38	460.42	460.42	279.65	279.65	419.38	1086.72	42.18	54.57	12.39	3.40
	R404a	362.77	391.51	391.51	271.29	271.29	362.77	1659.9	42.18	55.43	13.25	3.18
	R507	358.94	386.84	386.84	271.91	271.91	358.94	1744.78	42.18	55.70	13.52	3.12
Erzurum $T_{out} = 31\,°C$ $T_{cond} = 36\,°C$	R12	350.77	372.92	372.92	235.14	235.14	350.77	1013.09	32.54	38.77	6.23	5.22
	R22	402.65	433.23	433.23	244.43	244.43	402.65	740.387	32.54	38.83	6.29	5.17
	R134a	394.97	423.23	423.23	250.54	250.54	394.97	811.078	32.54	38.91	6.37	5.11
	R407c	406.57	438.69	438.69	245.63	245.63	406.57	727.874	32.54	39.03	6.49	5.01
	R410A	419.38	452.73	452.73	258.69	258.69	419.38	729.006	32.54	39.29	6.75	4.82
	R404a	362.77	386.51	386.51	252.65	252.65	362.77	1063.78	32.54	39.56	7.02	4.64
	R507	358.94	381.99	381.99	253.15	253.15	358.94	1107.33	32.54	39.63	7.09	4.59

where the temperature difference was the difference between the ceiling and inside temperatures.

$$\Delta T_{13} = T_{\mathrm{cl}} - T_{\mathrm{in}} \tag{9}$$

2.1.4 Heat Transfer Rate from Air Alteration (Q_{21})

Some amount of heat transfer occurred when the door of the cold room was opened to the outside or a place with a different temperature than the inside of the cold room. This situation brought an additional cooling load to the system, which was calculated as:

$$Q_{21} = H_{\mathrm{d}}\, V (h_{\mathrm{out}} - h_{\mathrm{in}}) \rho_{\mathrm{air}} \tag{10}$$

where the air alteration coefficient (H_{d}) was assumed to be 1.7 times/24 h for this application.

2.1.5 The Heat Transfer Rate from Preserved Products (Q_{31}, Q_{32}, Q_{33})

The cooling load from the preserved product can be evaluated in three sections, which are summarized below briefly. These sections depended upon the type of product. The specific heats of the pears before and after the freezing point are 3.61 and 1.88 $\mathrm{kJ\,kg^{-1}\,K^{-1}}$, respectively. The latent heat of freezing and the heat of respiration are 277 $\mathrm{kJ\,kg^{-1}}$ and 0.005 $\mathrm{W\,kg^{-1}}$ for pears.

First, the heat rejection rate from the preserved products for the temperature above the freezing temperature was calculated as:

$$Q_{31} = m C_{\mathrm{p1}} \Delta T_{31} \tag{11}$$

where the temperature difference was the same as in Eq. (5).

Second, the heat rejection rate from the preserved products during the freezing temperature was shown as:

$$Q_{32} = m_{\mathrm{p}}\, l \tag{12}$$

Third, the heat rejection rate from the preserved products was calculated after the freezing process as:

$$Q_{33} = m C_{\mathrm{p3}}\, \Delta T_{33} \tag{13}$$

where the temperature difference was the difference between the freezing temperature and the temperature after the freezing process.

$$\Delta T_{33} = T_{\mathrm{fp}} - T_{\mathrm{afp}} \tag{14}$$

2.1.6 The Heat Transfer Rate from the Heat Sources in the Cold Room (Q_{41}, Q_{42}, Q_{43}, Q_{44})

The duration of the cooling process was planned to be 20 h a day. The human working time, in other words, the illumination time was assumed to be 2 h a day for two individuals working in the cold room. The illumination was performed by four pieces of 100 W fluorescents. Each of four electric engines had 780 W of power in the case study. The heat transfers rates from the workers (Q_{41}), illumination (Q_{42}), electric engines (Q_{43}) and electric heater with defrost (Q_{44}) in the cold room were determined respectively as:

$$Q_{41} = n_{\mathrm{p}}\, t_{41}\, Q_{\mathrm{i}} \tag{15}$$

$$Q_{42} = W_1\, t_{42} \tag{16}$$

$$Q_{43} = n_{\mathrm{em}}\, W_2\, Q_{\mathrm{em}}\, t_{43} \tag{17}$$

$$Q_{44} = n_{\mathrm{eh}}\, W_3\, \mathrm{Ft}_{44} \tag{18}$$

2.2 Calculation Procedure for Energy Analysis

The state-point properties and results of energy equations below are presented in Table 4 as a case study. The heat transfer rate of the evaporator (Q_{evap}) and refrigerant charge rate, respectively, were calculated as follows:

$$Q_{\mathrm{CL}} = Q_{\mathrm{evap}} = m(h_1 - h_4) \tag{19}$$

$$m = \frac{Q_{\mathrm{CL}}}{h_1 - h_4} \tag{20}$$

The condenser capacity (Q_{cond}) and isentropic compression work of the compressor (W_{comp}), respectively, were expressed as follows:

$$Q_{\mathrm{cond}} = m(h_2 - h_3) \tag{21}$$

$$W_{\mathrm{comp}} = m(h_2 - h_1) \tag{22}$$

The efficiency of a refrigerator is expressed in terms of the COP. It is the ratio of the heat removed from the space to be refrigerated to the work to be consumed to accomplish this task. As the COP value rises, power consumption decreases. It is obvious that this situation will help to reduce the environmental pollution caused by power production systems. The COP of the refrigeration system's cycle can be determined by the following equation:

$$\mathrm{COP} = \frac{Q_{\mathrm{evap}}}{W_{\mathrm{comp}}} \tag{23}$$

2.3 Calculation Procedure for Exergy Analysis

Energy and exergy analyses were used in this subsection to conduct thermodynamic performance comparisons. Many researchers have proposed that the thermodynamic performance of a process is best evaluated using exergy analysis [18,19]. Exergy is the maximum amount of work that can be produced by a stream or a system as it is brought into equilibrium with a reference environment. It can be thought of as a measure of the usefulness or quality of energy. Exergy is consumed during real processes and conserved during ideal

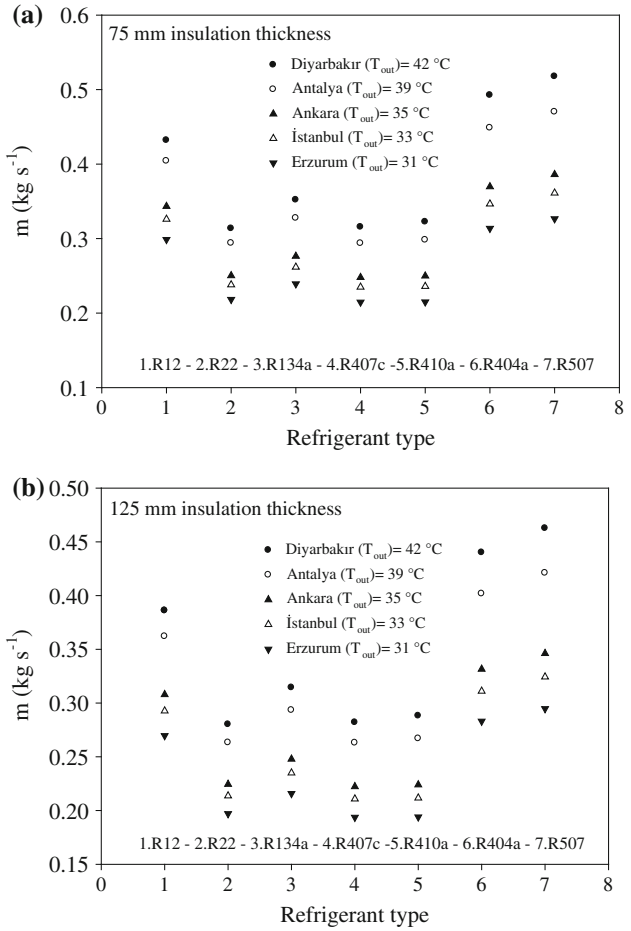


Fig. 2 Alteration of the refrigerant charge rate obtained by Eq. (20) according to the investigated cities of Turkey and refrigerant types

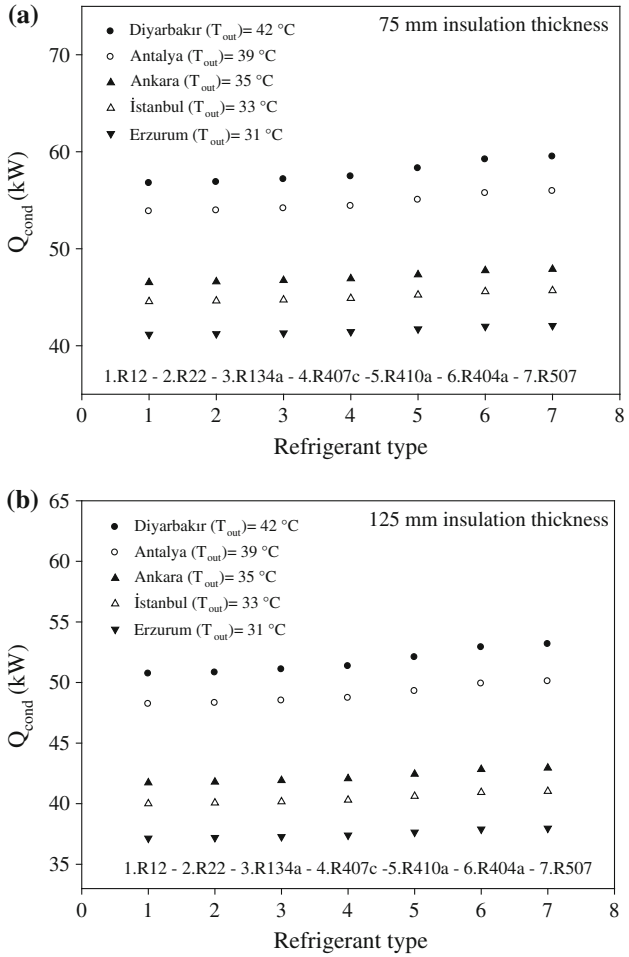


Fig. 3 Alteration of the condenser capacity obtained by Eq. (21) according to the investigated cities of Turkey and refrigerant types

processes. In general, energy and exergy efficiencies are calculated as the ratio of the energy (or exergy) of the product(s) to the energy (or exergy) of the input(s). The exergy balance of the refrigeration system was calculated in a steady state. Neglecting the kinetic, chemical and potential energies and the balances of mass, energy and exergy were used for the determination of heat input, rate of exergy loss and efficiency of exergy in this study. The mass balance and exergy balance equations are shown in the following equations:

$$\sum_{\text{in}} m - \sum_{\text{out}} m = 0 \tag{24}$$

$$E_{\text{Q}} - E_{\text{W}} = \sum_{\text{out}} \text{me} + \sum_{\text{in}} \text{me} + I \tag{25}$$

where I is the rate of irreversibility (or the rate of exergy destruction, $I = T_{\text{os}}$), m_{e} is the exergy flow rate of working fluid, E_{Q} is the rate of exergy of heat input, E_{W} is the rate of exergy of power output and s_{gen} is the rate of entropy generation. The rate of heat exergy and the power exergy, respectively, were defined in the following equations:

$$E_{\text{Q}} = Q\left(1 - \frac{T_0}{T}\right) \tag{26}$$

$$E_{\text{W}} = W \tag{27}$$

The exergy rate at the state points in Fig. 1 was calculated as:

$$E_{\text{i}} = m\left[(h_{\text{i}} - T_0 s_{\text{i}}) - (h_0 - T_0 s_0)\right] \tag{28}$$

The exergy analysis for each component of the refrigeration cycle in Fig. 1 was summarized from Eqs. (29) to (40). The exergy rate balance, irreversibility and exergy efficiency for the compressor (i.e., processes 1–2) are shown in Eqs. (29), (30), and (31), respectively.

$$\text{me}_1 = E_{\text{W}} + \text{me}_2 + I_{\text{comp}} \tag{29}$$

$$I_{\text{comp}} = mT_0(s_2 - s_1) \tag{30}$$

$$\eta_{\text{comp}} = \frac{E_2 - E_1}{W_{\text{comp}}} \tag{31}$$

The exergy rate balance, irreversibility and exergy efficiency for the condenser (i.e., processes 2–3) are shown in Eqs. (32), (33), and (34), respectively:

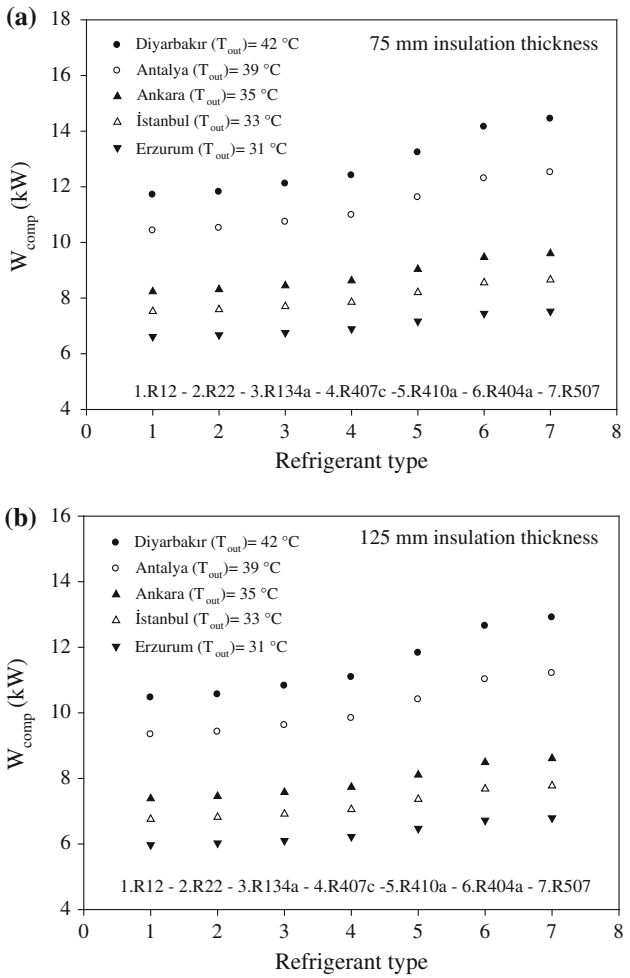


Fig. 4 Alteration of the compressor work obtained by Eq. (22) according to the investigated cities of Turkey and refrigerant types

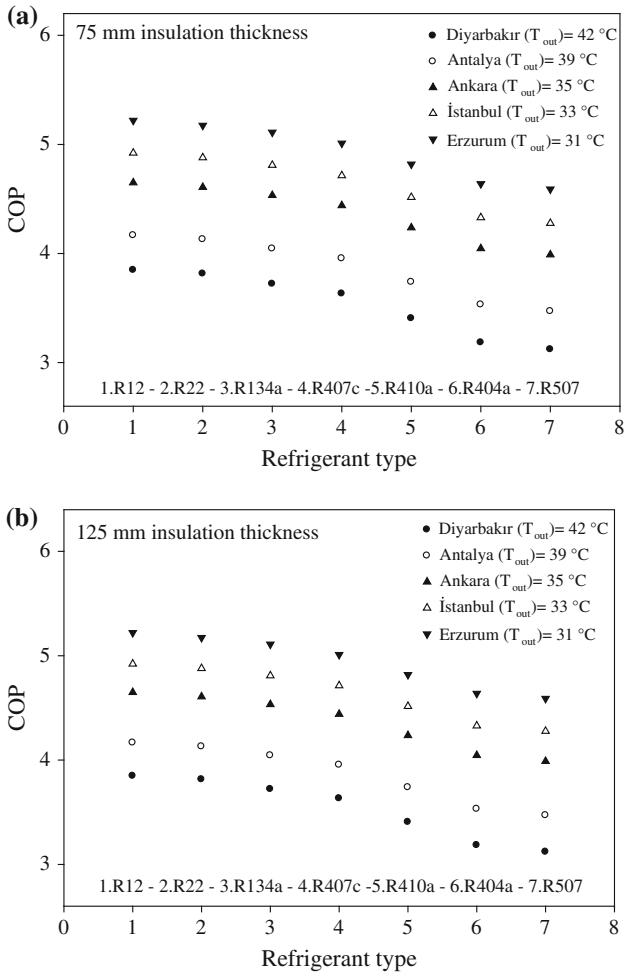


Fig. 5 Alteration of the COP obtained by Eq. (23) according to the investigated cities of Turkey and refrigerant types

$$\mathrm{me}_2 = E_{\mathrm{Q,cond}} + \mathrm{me}_3 + I_{\mathrm{cond}} \tag{32}$$

$$I_{\mathrm{cond}} = m\left[(h_2 - h_3) - T_0(s_2 - s_3)\right] \tag{33}$$

$$\eta_{\mathrm{cond}} = \frac{E_3}{E_2} \tag{34}$$

The exergy rate balance, irreversibility and exergy efficiency for the throttling valve (i.e., processes 3–4) are shown in Eqs. (35), (36), and (37), respectively:

$$\mathrm{me}_3 = \mathrm{me}_4 + I_{\mathrm{tv}} \tag{35}$$

$$I_{\mathrm{tv}} = mT_0(s_4 - s_3) \tag{36}$$

$$\eta_{\mathrm{tv}} = \frac{E_4}{E_3} \tag{37}$$

The exergy rate balance, irreversibility and exergy efficiency for the evaporator (i.e., processes 4–1) are shown in Eqs. (38), (39), and (40), respectively:

$$\mathrm{me}_4 + E_{\mathrm{Q,evap}} = \mathrm{me}_1 + I_{\mathrm{evap}} \tag{38}$$

$$I_{\mathrm{evap}} = m\left[(h_4 - h_1) - T_0(s_4 - s_1)\right] \tag{39}$$

$$\eta_{\mathrm{tv}} = \frac{E_1}{E_4} \tag{40}$$

The total refrigeration cycle's irreversibility rate can be expressed as:

$$I_{\mathrm{TOTAL}} = I_{\mathrm{comp}} + I_{\mathrm{cond}} + I_{\mathrm{tv}} + I_{\mathrm{evap}} \tag{41}$$

Efficiency defect is a significant parameter in analyses of multicomponent thermal systems. Fractions of input are lost through irreversibilities. They can be calculated as efficiency defects [20] in Eq. (42):

$$\delta_i = \frac{I_i}{W_{\mathrm{comp}}} \tag{42}$$

Detailed information on the subject of thermodynamics of exergy analysis can be found in Bejan's works [21,22].

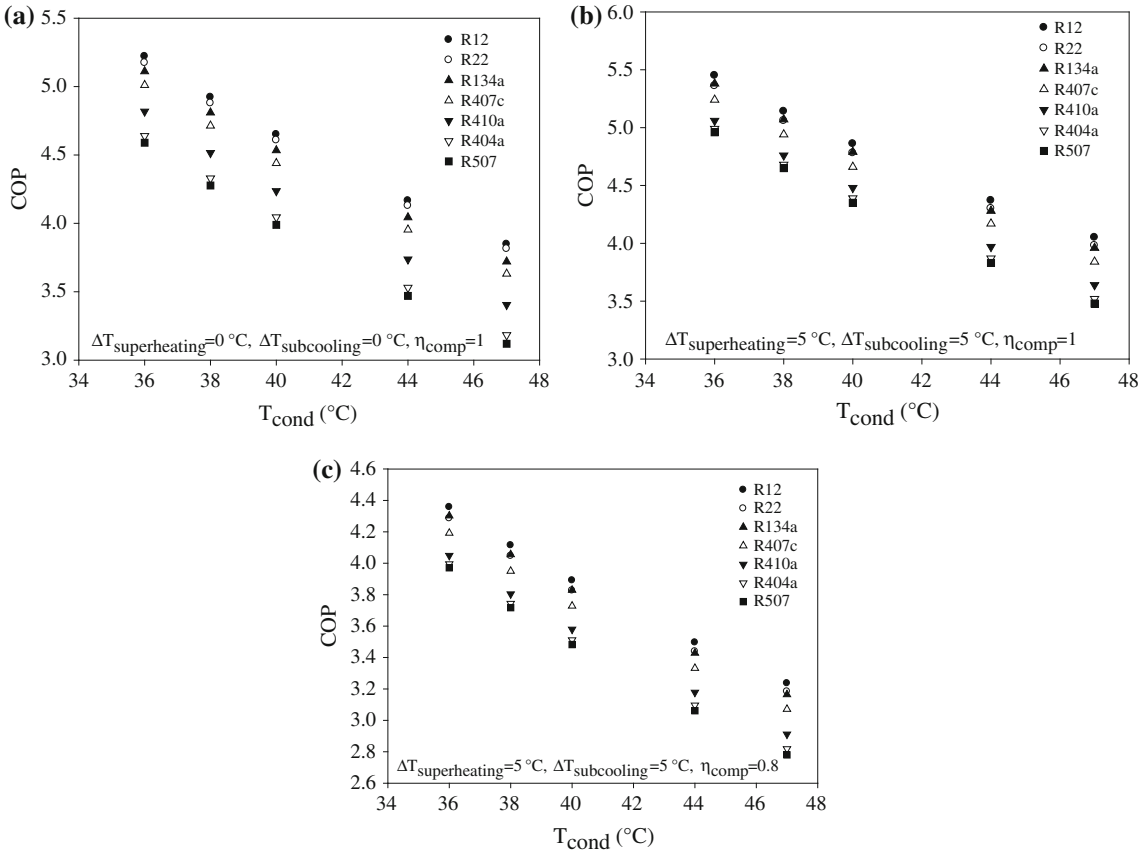


Fig. 6 Coefficient of performance (**a**–**c**) versus condensing temperature

3 Results and Discussion

This paper included a description of a theoretical model and its application on the design of a cold room using Turkey as a case study. The investigated model can be used to assess the completeness and effectiveness of cold-room systems with regard to heat transfer and thermodynamics analyses for the basic components of the single-stage vapor-compression refrigeration cycle. The effective cooling of approximately −40 °C can be obtained with the use of a single-stage vapor compression refrigeration system. Efficiency begins to decrease at temperatures below −35 °C due to a large difference between the evaporator and the condenser temperatures. The evaporating temperature was held constant at −6 °C due to the preserved products. For that reason, the single-stage vapor compression system was supposed to correspond to the necessary performance issues. A cascade refrigeration system should be utilized to work with a lower temperature than −40 °C.

Thermodynamic efficiency is determined by first-law energy analysis, which can be used to compare alternative cycles. The determination of COP is performed for this purpose. Irreversibilities cause reductions in the cycle's COP, and the minimization of irreversibilities increases the cycle's efficiency. These irreversibilities' places as components in the refrigeration cycle and their magnitudes cannot be detected by first-law energy analysis. Second-law exergy analysis can handle this problem. Stegou-Sagia and Paignigiannia [23] emphasized that exergy analysis was a dominant method in the design, optimization and performance estimation of the refrigeration cycle.

The general characteristics of energy analyses are listed in Figs. 2, 3, 4, 5, which show either the effect of alterations of outside temperatures in different cities or the effect of the use of various refrigerants and alterations of insulation thickness of the cold room on the refrigerant charge rate, condenser capacity, compressor work and COP. Figure 2 shows that the refrigeration charge rate decreases with increases in the insulation thickness. The highest use of refrigerant charge rate was in the city of Diyarbakır, which has a higher outside temperature than the other cities examined. Further, R410A and R407C have the lowest refrigerant charge rate values together with R22. Figures 3 and 4 show that the condenser capacity and the compressor work have a similar pattern. That is, they decrease with increasing insulation thickness from 75 to 125 mm and increase with increasing outside temperatures of the cold room from 36 to 47 °C or condenser temperatures from 36 to 47 °C. Figure 5 shows the alteration of COP values

Table 5 Sample case study for the comparison of various refrigerants according to the components of refrigeration cycle for Istanbul ($T_{out} = 33\,^{\circ}C$, $T_{cond} = 38\,^{\circ}C$, $Q_{evap} = 33.25\,kW$) at the fixed temperature of $T_{CR} = -1\,^{\circ}C$, $T_{evap} = -6\,^{\circ}C$, $\Delta T_{subcooling} = 5\,^{\circ}C$, $\Delta T_{superheating} = 5\,^{\circ}C$ and $\eta_{comp} = 0.8$, $T_o = T_{out} = 33\,^{\circ}C$

Compressor								Condenser							
Refrigerant	e_1 (kJ kg^{-1})	e_2 (kJ kg^{-1})	E_1 (kW)	E_2 (kW)	I (kW)	δ	η_E (%)	Refrigerant	e_2 (kJ kg^{-1})	e_3 (kJ kg^{-1})	E_2 (kW)	E_3 (kW)	I (kW)	δ	η_E (%)
R12	98.21	122.24	1.37	1.7	0.07683	0.186	81.35	R12	122.25	119.22	1.71	1.66	0.04223	0.102	97.52
R22	90.46	124.08	0.925	1.26	0.07484	0.178	82.13	R22	124.09	118.99	1.27	1.22	0.05218	0.124	95.89
R134a	91.54	122.19	1.013	1.35	0.07861	0.188	81.19	R134a	122.19	118.78	1.35	1.32	0.03782	0.09	97.21
R407c	86.66	121.77	0.864	1.21	0.07877	0.183	81.64	R407c	121.78	119.00	1.22	1.19	0.02774	0.064	97.72
R410A	87.77	124.62	0.869	1.23	0.08036	0.18	81.96	R410A	124.62	118.78	1.24	1.18	0.05797	0.13	95.31
R404a	95.96	121.88	1.36	1.72	0.08545	0.188	81.12	R404a	121.88	119.07	1.73	1.69	0.03989	0.088	97.69
R507	96.73	121.89	1.42	1.79	0.08633	0.189	81.06	R507	121.89	118.87	1.79	1.75	0.04451	0.097	97.52
Throttling valve								Evaporator							
Refrigerant	e_3 (kJ kg^{-1})	e_4 (kJ kg^{-1})	E_3 (kW)	E_4 (kW)	I (kW)	δ	η_E (%)	Refrigerant	e_4 (kJ kg^{-1})	e_1 (kJ kg^{-1})	E_4 (kW)	E_1 (kW)	I (kW)	δ	η_E (%)
R12	119.22	115.85	1.66	1.62	0.04695	0.113	97.18	R12	115.85	98.22	1.62	1.37	0.24605	0.597	84.78
R22	118.99	114.52	1.22	1.17	0.04572	0.109	96.25	R22	114.52	90.46	1.17	0.93	0.24622	0.588	78.99
R134a	118.78	113.76	1.32	1.26	0.05557	0.132	95.77	R134a	113.76	91.54	1.26	1.01	0.24603	0.589	80.47
R407c	119.00	113.55	1.19	1.13	0.05435	0.126	95.42	R407c	113.55	86.66	1.13	0.86	0.26830	0.625	76.32
R410A	118.78	112.63	1.18	1.12	0.06096	0.136	94.82	R410A	112.63	87.77	1.12	0.87	0.24630	0.553	77.93
R404a	119.07	113.41	1.69	1.61	0.08025	0.177	95.25	R404a	113.41	95.97	1.61	1.36	0.24718	0.546	84.62
R507	118.87	113.42	1.75	1.67	0.08004	0.175	95.42	R507	113.42	96.74	1.67	1.42	0.24511	0.538	85.29

Table 6 Sample case study for the comparison of various refrigerants according to the components of refrigeration cycle for Istanbul ($T_{out} = 33\,^{\circ}C$, $T_{cond} = 38\,^{\circ}C$, $Q_{evap} = 33.25\,kW$) at the fixed temperature of $T_{CR} = -1\,^{\circ}C$, $T_{evap} = -6\,^{\circ}C$, $\Delta T_{subcooling} = 5\,^{\circ}C$, $\Delta T_{superheating} = 5\,^{\circ}C$ and $\eta_{comp} = 0.8$, $T_0 = 25\,^{\circ}C$

Compressor								Condenser							
Refrigerant	e_1 (kJ kg^{-1})	e_2 (kJ kg^{-1})	E_1 (kW)	E_2 (kW)	I (kW)	δ	η_E (%)	Refrigerant	e_2 (kJ kg^{-1})	e_3 (kJ kg^{-1})	E_2 (kW)	E_3 (kW)	I (kW)	δ	η_E (%)
R12	83.14	107.32	1.16	1.50	0.07482	0.182	81.84	R12	107.32	100.42	1.50	1.40	0.09622	0.234	93.57
R22	76.96	110.78	0.79	1.13	0.07288	0.174	82.60	R22	110.78	100.42	1.13	1.03	0.10609	0.253	90.64
R134a	77.83	108.67	0.86	1.20	0.07656	0.183	81.69	R134a	108.67	100.35	1.20	1.11	0.09208	0.220	92.35
R407c	73.39	108.71	0.73	1.08	0.07672	0.179	82.12	R407c	108.71	100.44	1.08	1.00	0.08255	0.192	92.39
R410A	74.82	111.88	0.74	1.11	0.07827	0.176	82.44	R410A	111.88	100.54	1.11	1.00	0.11243	0.252	89.86
R404a	81.32	107.39	1.15	1.52	0.08322	0.184	81.62	R404a	107.39	100.68	1.52	1.43	0.09501	0.210	93.76
R507	81.97	107.27	1.20	1.58	0.08408	0.184	81.56	R507	107.27	100.50	1.58	1.48	0.09959	0.218	93.68
Throttling valve								Evaporator							
Refrigerant	e_3 (kJ kg^{-1})	e_4 (kJ kg^{-1})	E_3 (kW)	E_4 (kW)	I (kW)	δ	η_E (%)	Refrigerant	e_4 (kJ kg^{-1})	e_1 (kJ kg^{-1})	E_4 (kW)	E_1 (kW)	I (kW)	δ	η_E (%)
R12	100.42	97.14	1.40	1.36	0.04572	0.111	96.74	R12	97.14	83.14	1.36	1.16	0.24605	0.597	85.59
R22	100.42	96.06	1.03	0.98	0.04452	0.106	95.67	R22	96.06	76.96	0.98	0.79	0.24622	0.588	80.12
R134a	100.35	95.47	1.11	1.06	0.05412	0.129	95.13	R134a	95.47	77.83	1.06	0.86	0.24603	0.589	81.53
R407c	100.44	95.13	1.00	0.95	0.05292	0.123	94.72	R407c	95.13	73.39	0.95	0.73	0.26830	0.625	77.14
R410A	100.54	94.55	1.00	0.94	0.05936	0.133	94.04	R410A	94.55	74.82	0.94	0.74	0.24630	0.553	79.13
R404a	100.68	95.17	1.43	1.35	0.07815	0.173	94.52	R404a	95.17	81.32	1.35	1.15	0.24718	0.546	85.44
R507	100.50	95.19	1.48	1.40	0.07795	0.171	94.72	R507	95.19	81.97	1.40	1.20	0.24511	0.538	86.11

Table 7 Irreversibility rates for the stated values of T_{cond} for the comparison of investigated refrigerants at the fixed temperature of $T_{CR} = -1\,^{\circ}C$, $T_{evap} = -6\,^{\circ}C$, $\Delta T_{subcooling} = 5\,^{\circ}C$, $\Delta T_{superheating} = 5\,^{\circ}C$ and $\eta_{comp} = 0.8$

Investigated cities of Turkey	T_{cond} (°C)	Q_{evap} (kW)	Total irreversibility rates (kW)						
			R12	R22	R134a	R407c	R410a	R404a	R507
$T_o = T_{out}$									
Diyarbakır	47	40.25	0.52389	0.53257	0.53575	0.55199	0.5822	0.60144	0.60970
Antalya	44	38.88	0.48495	0.49298	0.49445	0.50884	0.53341	0.54746	0.55369
Ankara	40	34.34	0.43573	0.44302	0.44272	0.45473	0.47359	0.48268	0.48680
İstanbul	38	33.25	0.41206	0.41895	0.41803	0.42915	0.44559	0.45277	0.456
Erzurum	36	31.18	0.38903	0.39557	0.39406	0.40437	0.41867	0.4243	0.42689
$T_0 = 25\,^{\circ}C$									
Diyarbakır	47	40.25	0.63177	0.64045	0.64359	0.66109	0.69008	0.70934	0.71751
Antalya	44	38.88	0.573778	0.581812	0.583263	0.598689	0.62224	0.63632	0.642473
Ankara	40	34.34	0.49918	0.50647	0.50617	0.51890	0.53705	0.54616	0.55022
İstanbul	38	33.25	0.46282	0.46972	0.46879	0.48049	0.49636	0.50356	0.50673
Erzurum	36	31.18	0.42711	0.43364	0.43213	0.44288	0.45675	0.46240	0.46495

with the investigated refrigerants. COP was found to increase with decreasing outside temperatures or condenser temperature. In addition, the insulation thickness of the cold room has no significant effect on the COP of the refrigerant cycle. R12 and R22 have the highest COP values, whereas R404A and R507 have the lowest values.

Cycle performance can be improved by the subcooling and superheating application. In this paper, the effects of the degree of subcooling and superheating were calculated respectively. A comparison was made between the superheating/subcoolingcase in Fig. 1b with the non-superheating/subcooling case in Fig. 1a. It is illustrated from Fig. 6a–c for the investigated refrigerants. Figure 6 shows the effect of assumed values of superheating, subcooling and compressor efficiency cases on the COP step by step. The ideal situation for the single-stage refrigeration cycle is presented for comparison in Fig. 6a. The case of subcooling and superheating, assuming that compressor isentropic efficiency was 100 %, caused increase in COP (see Fig. 6b). The improvement was due to the increase in the compressor inlet temperature, which increased the compressor power (W_{comp}) and performance coefficient. The cycle performance was affected by the subcooling more than the superheating. On the other hand, Fig. 6c shows that compressor isentropic efficiency was more dominant than the subcooling and superheating cases on COP. In a real system, compressor isentropic efficiency is a function of the evaporator and condenser pressures. The real refrigerating capacity and COP can be calculated if the efficiency of the compressor is known. The refrigerating capacity is influenced by the volumetric efficiency and COP by the isentropic efficiency. Despite the increase in COP by means of the subcooling and superheating cases in Fig. 6b, the assumed compressor isentropic efficiency caused decrease in COP values lower than those in Fig. 6a, b.

From Tables 4, 5, 6, 7, significant parameters of cycle performance under different conditions are calculated as case studies of the investigated refrigerants for the same evaporation temperature related to the preserved products. In addition, the evaluation of cycle performance results under different working conditions was consistent with those under real working conditions.

Table 4 shows a case study to determine the characteristic parameters of the energy analyses for the specific conditions of selected Turkish cities. Diyarbakır had the highest outside temperature and condenser temperatures (42 and 47 °C, respectively). Erzurum had the lowest outside temperature and condenser temperatures (31 and 36 °C, respectively). Ideal conditions for the components of the refrigeration system were used to show the effect of the use of various refrigerants on the required refrigerant charge rate, capacity of the condenser, required compressor work and COP for a constant insulation thickness of 100 mm and a constant cooling load (i.e., a constant evaporating temperature). As a result, the high performance refrigerants were put in order according to their COP values. As seen in Table 4, traditional refrigerants have higher COP values than alternative refrigerants. The refrigerant charge rates of R134A, R407C, R410A and R404A are similar to that of R22, whereas R507 has the lowest COP value and highest refrigerant charge rate. The comparison of the refrigeration systems in the cities of Erzurum and Diyarbakır demonstrates the effect of the outside temperature on the preservation of the same product in a cold room. The low outside temperature condition (Erzurum) has

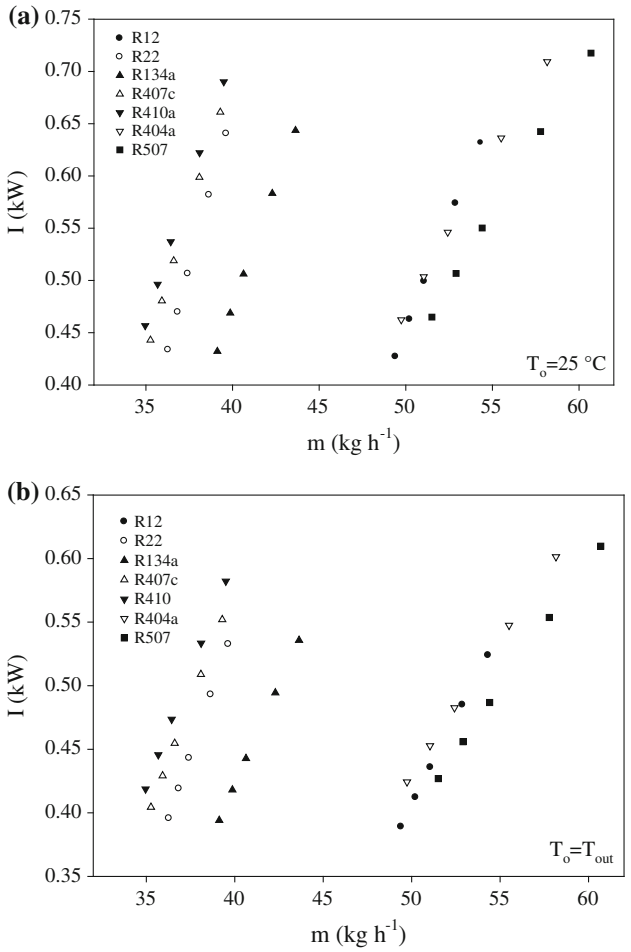


Fig. 7 Total irreversibilities versus refrigerant charge rate for all investigated cities at the fixed temperature of $T_{CR} = -1\,^{\circ}C$, $T_{evap} = -6\,^{\circ}C$, $\Delta T_{subcooling} = 5\,^{\circ}C$, $\Delta T_{superheating} = 5\,^{\circ}C$ and $\eta_{comp} = 0.8$, $T_0 = 25\,^{\circ}C$

higher COP values and lower refrigerant charge rate values than the high outside temperature condition (Diyarbakır) in the case study.

Tables 5 and 6 illustrate the difference in the use of reference temperature and its effect on each component of the refrigeration cycle. First, the reference temperature was equal to the outside temperature of the cold room (see Table 5) and assumed to be 25 °C, which is commonly done in the literature. As a result, the losses in the evaporator seemed important with their large and constant values apart from the others. In addition, exergetic efficiencies of the condenser and throttling valve were found to be higher than those of other components. Tables 5 and 6 also show the exergy performance of the investigated refrigerants for each component of the refrigeration cycle.

The irreversibility rates of all the investigated refrigerants were plotted against the refrigerant charge rates in Fig. 7, according to the alteration of the reference temperature. The largest irreversibility rate and refrigerant charge rate were seen in R507 and R404A. As shown in Fig. 7, the refrigerant charge rate increased with the irreversibility rate. Moreover, when the reference temperature was assumed to be 25 °C, as shown in Fig. 7a, the irreversibility values were found to be higher than of those in Fig. 7b, which shows the reference temperature as the outside temperature of the cold room. This situation regarding the increase in irreversibility values can also be clearly seen in Table 7. That is, the total irreversibility rates increased with increasing condenser temperatures.

The efficiency defects in the components of the refrigerating cycle in Fig. 1 are shown in Fig. 8 for all of the investigated refrigerants. The maximum efficiency defect was found in the evaporator in comparison to other components, followed by the condenser, compressor and refrigerant expansion valve. The efficiency defects for R407C and R410A were also the maximum values in the evaporator. These findings associated with the efficiency defects indicate that design improvements of components are needed to enhance the exergetic efficiency of the single-stage refrigeration system.

The thermodynamic analysis of CFC-12, HCFC-22 and their alternatives, such as HFC-134A, HFC-404A, HFC-407C, HFC-410A and HFC-507 was studied by both the first and the second laws of thermodynamics using the single-stage vapor-compression refrigeration cycle. The analysis was performed on each of the system components to determine their individual roles in the overall system of irreversible losses. Most of the losses were found to be due to the evaporator. The irreversibility of the condenser was also significant.

4 Conclusion

A thermodynamic energy and exergy analysis to optimize a single-stage vapor-compression refrigeration system to be used for a cold-storage application was presented in this paper. Its fundamental issues were discussed in detail. Many case studies with different theoretical conditions were described to determine the optimum operating conditions for the preservation of pears.

The proposed model provided a useful procedure for the cold-room project design. It is expected that it will be a beneficial source for researchers interested in the topic of refrigeration and air conditioning. The results of this study are of technological importance for efficient design when cold-room systems are assigned to utilize various alternative refrigerants in different regions of Turkey.

An ideal vapor compression refrigeration system was used for the performance analysis of alternative new refrigerants as substitutes for CFC-12, HFC134A and CFC-22. Considering the comparison of COP and refrigerant charge rates of the tested refrigerants, refrigerants of R407C and

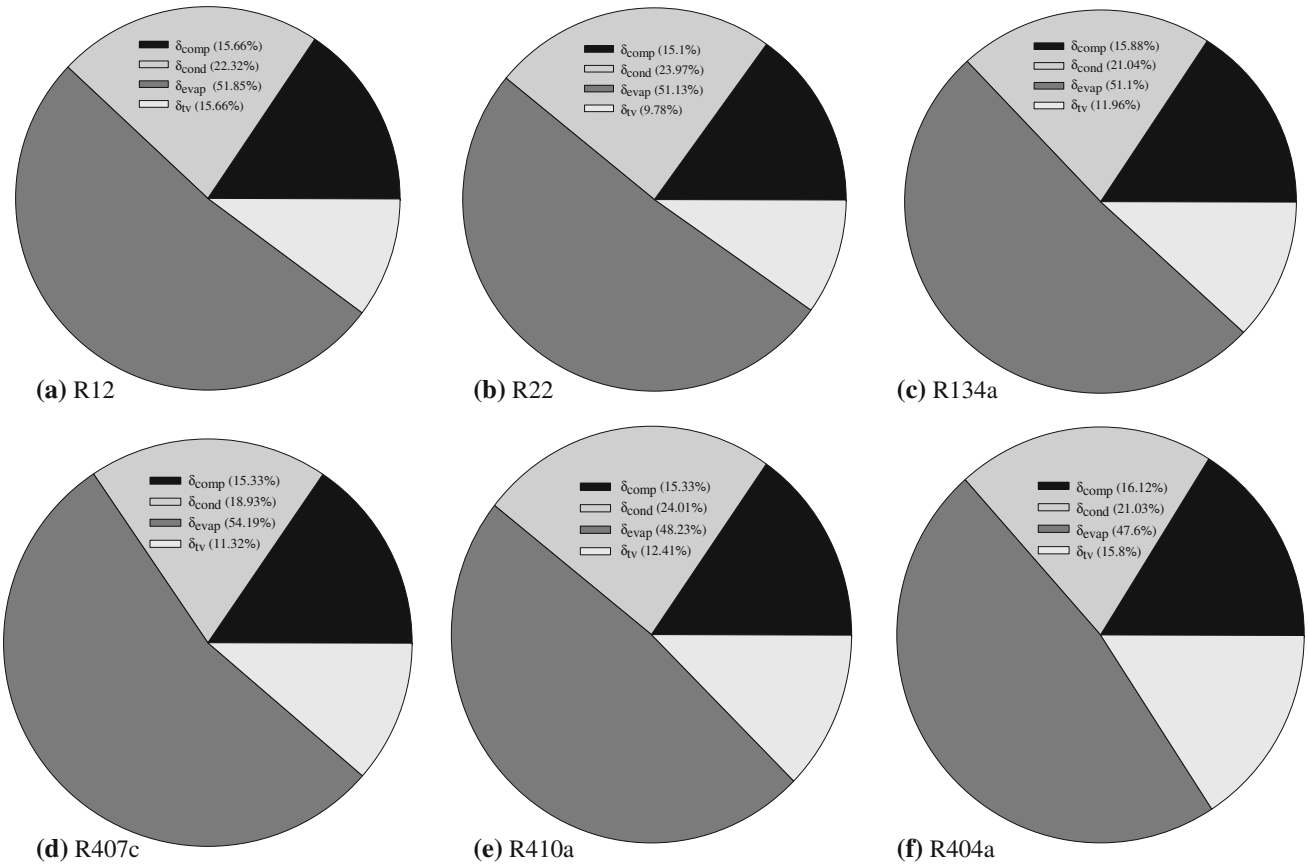


Fig. 8 Pie chart of efficiency defects of the investigated refrigerants belong to Ankara city for a condenser temperature of 40 °C and the fixed temperature of $T_{CR} = -1\,°C$, $T_{evap} = -6\,°C$, $\Delta T_{subcooling} = 5\,°C$, $\Delta T_{superheating} = 5\,°C$ and $\eta_{comp} = 0.8$, $T_o = 25\,°C$

R410A were found to be the most suitable alternatives among refrigerants tested for R12 and R22, respectively. The COP of the system decreased with increasing condensing temperature for a constant evaporating temperature in the analysis. All systems were improved by analyzing the effect of the superheating/subcooling case. Further, the effect of compressor efficiency on COP was also discussed in various case studies.

The analysis of the single-stage vapor-compression refrigeration cycle's performance by the exergy method illustrates the utility of this method. Employing the concept of efficiency defect enabled the ratios of input lost through irreversibilities and demonstrated the components of the refrigeration system needed to optimize the specified preservation conditions of the product. A large amount of exergy is wasted during the working of the system, which decreases the exergy efficiency of the refrigeration system.

There is not any refrigerant that meets all of the necessary requirements due to the changes in the thermodynamic physical properties of the refrigerant. The thermo-physical properties, such as performance and efficiency, limitations and restrictions related to safety, environmental impact and associated legislation, are the most significant factors in choosing a new refrigerant. Low viscosities of liquid and vapor phases, high liquid specific heat, high thermal conductivities of liquid and vapor phases, high latent heat, and limited temperature glide are the desired thermo-physical properties of refrigerant/refrigerant mixtures.

Acknowledgments The authors are indebted to the Departments of Mechanical Engineering, Yildiz Technical University (YTU) and King Mongkut's University of Technology Thonburi (KMUTT) for supporting this study. The first author wishes to thank King Mongkut's University of Technology Thonburi (KMUTT) for providing him with a postdoctoral fellowship. The fourth author would like to thank the Thailand Research Fund for the support.

References

1. Lee, Y.S.; Su, C.C.: Experimental studies of isobutane (R600a) as the refrigerant in domestic refrigeration system. Appl. Thermal Eng. **22**, 507–519 (2002)
2. Devotta, S.; Gopichand, S.; Pendyola, V.R.: Assessment of HFCs, fluorinated ethers and amine as alternatives to CFC 12. Int. J. Refrig. **16**, 84–89 (1993)
3. Wongwises, S.; Kamboon, A.; Orachon, B.: Experimental investigation of hydrocarbon mixtures to replace HFC-134a in an automotive air conditioning system. Energy Convers. Manag. **47**, 1644–1659 (2006)

4. Wongwises, S.; Chimres, N.: Experimental study of hydrocarbon mixtures to replace HFC-134a in a domestic refrigerator. Energy Convers. Manag. **46**, 85–100 (2005)
5. Wongwises, S.; Pirompak, W.: Flow characteristics of pure refrigerants and refrigerant mixtures in adiabatic capillary tubes. Appl. Thermal Eng. **21**, 845–861 (2001)
6. Wongwiscs, S.; Songnetichaovalit, T.; Lokathada, N.; Kritsadathikarn, P.; Suchatawat, M.; Pirompak, W.: A comparison of the flow characteristics of refrigerants flowing through adiabatic capillary tubes. Int. Commun. Heat Mass Transf. **27**, 611–621 (2000)
7. Dalkilic, A.S.; Wongwises, S.: A performance comparison of vapour-compression refrigeration system using various alternative refrigerants. Int. Commun. Heat Mass Transf. **37**(9), 1340–1349 (2010)
8. Dalkilic, A.S.; Wongwises, S.: Comparison of various alternative refrigerants for vapour compression refrigeration systems. In: Proceedings of the ASME/JSME 8th Thermal Engineering Joint Conference, March 13–17, USA (2011)
9. Dalkilic, A.S.: Theoretical analysis on the prediction of performance coefficient of two-stage cascade refrigeration system using various alternative refrigerants. Isi BilimiveTeknigiDergisi/J. Thermal Sci. Technol. (2012) (in Press)
10. Dopazo, J.A.; Fernández-Seara, J.; Sieres, J.; Uhía, F.J.: Theoretical analysis of a CO_2–NH_3 cascade refrigeration system for cooling applications at low temperatures. Appl. Thermal Eng. **29**, 1577–1583 (2009)
11. Lee, Y.S.; Su, C.C.: Experimental studies of isobutane (R600a) as the refrigerant in domestic refrigeration system. Appl. Thermal Eng. **22**, 507–519 (2002)
12. Kanoğlu, M.: Exergy analysis of multistage cascade refrigeration cycle used for natural gas liquefaction. Int. J. Energy Res. **26**, 763–774 (2002)
13. Cengel, Y.; Boles, M.A.: Thermodynamics—An Engineering Approach. McGraw-Hill, New York (2010)
14. REFPROP, Thermodynamic properties of refrigerants and refrigerant mixtures, version 7, Gaithersburg, M.D. National Institute of Standards and Technology (2001)
15. SOLKANE Refrigerant software, version 7, Hannover, Solvay Fluor Gmbh (2010)
16. Duruk, A.M.; Sarıbatı, Ş.: Soğutmatesisatı, TMMOB, publication number MMO/295-2 (2002)
17. Özkol, N.: Uygulamalısoğutmatekniği, TMMOB, publication number MMO/115-7 (1999)
18. Stegou-Sagia, A.; Paignigiannis, N.: Evaluation of mixtures efficiency in refrigerating systems. Energy Convers. Manag. **46**, 2787–2802 (2005)
19. Arcaklıoglu, E.; Cavusoglu, A.; Erisen, A.: Thermodynamic analysis of refrigerant mixtures for possible replacements for CFCs by an algorithm compiling property data. Appl. Thermal Eng. **26**, 430–439 (2006)
20. Kopac, M.; Zehmer, B.: Effect of saturation-temperature on the performance of a vapour-compression refrigeration-cycle working on different refrigerants using exergy method. Int. J. Energy Res. **30**, 729–740 (2006)
21. Bejan, A.: Advanced Engineering Thermodynamics, 3rd edn. Wiley, Hoboken, New York (2006)
22. Bejan, A.: Entropy Generation Minimization. CRC Press, Boca Raton (1996)
23. Stegou-Sagia, A.; Paignigiannia, N.: Exergy losses in refrigerating systems. A study for performance comparisons in compressor and condenser. Int. J. Energy Res. **27**, 1067–1078 (2003)